Journal of Nuclear Materials 399 (2010) 219–224

Contents lists available at ScienceDirect

Journal of Nuclear Materials

journal homepage: www.elsevier.com/locate/jnucmat

Identification of new phases in annealed Fe–18CrWTi ODS powders

C. Cayron [a,*], A. Montani [a], D. Venet [a], Y. de Carlan [b]

[a] CEA, LITEN, DTH, Minatec, 38054 Grenoble, France
[b] CEA, DEN, SRMA, 91191 Gif-sur-Yvette, France

ARTICLE INFO

Article history:
Received 5 December 2009
Accepted 27 January 2010

ABSTRACT

Fe–18CrWTi ODS steels are developed by CEA for the SFR generation IV program. The powders of a Fe–18CrWTi alloy reinforced by Y_2O_3 by mechanical milling have been annealed at 850 °C, 1100 °C and 1300 °C and their microstructure has been studied by SEM and TEM in order to better understand the precipitation mechanisms. The powders are constituted of large micrometric grains surrounded by nanometric ferritic grains. At 850 °C, no nano-oxide could be detected. At 1100 °C, some $Y_2Ti_2O_7$ precipitates of several hundreds of nanometres are detected at the grains boundaries, but again no nano-oxide could be observed. At 1300 °C, the precipitation has greatly changed. The sample contains hexagonal plate-shaped micrometric Y_2TiO_5 precipitates. A high density of nano-oxides of size around 20–30 nm is also revealed by EFTEM and HRTEM. They are of different types such as Y_2O_3, $Y_2Ti_2O_7$ and a new phase containing Y, Ti and O that we called PyrOrtho (orthorhombic with a = 7.24 Å, b = 12.4 Å and c = 18.2 Å). This study shows that addition of Ti makes the precipitation sequence very complex.

1. Introduction

CEA has decided to develop new oxide dispersion-strengthened (ODS) steels for the cladding tubes of the sodium fast reactors (SFR) developed in the framework of generation IV program. Fe–13/18CrWTi alloys reinforced by Y_2O_3 are developed in collaboration with A&D and Plansee. The steels are prepared by mechanical alloying, hot extrusion and hot rolling. The first results are promising [1] and further studies on the microstructure, workability, corrosion, welding and irradiation resistance of these materials are being performed.

Most of the interesting properties of the ODS steels are given by the nano-oxide dispersion. Understanding their formation is therefore the key to better control the microstructure and to improve the mechanical properties. The oxides are formed by a complex process. The initial Y_2O_3 particles of size between 50 and 100 nm are dissolved during the milling process, or at least are reduced to nanocluster sizes, and they re-precipitate as nano-oxides during the consolidation process [2–5]. The elements in the steels play a crucial role on the re-precipitation mechanism and on the product phases. Mn is incorporated inside the Y_2O_3 nano-precipitate without changing the crystallography, and V and Cr form oxide shells [6]. Ti has a more dramatic effect. It leads to a finer and denser precipitation of complex mixed Y_2O_3–TiO_2 nano-oxides [7]. X-ray diffraction on ODS steel powders containing high amounts of Y_2O_3 and Ti, milled at different times and annealed up to 1300 °C, proved that the complex nano-oxides are $Y_2Ti_2O_7$ and Y_2TiO_5 [2]. Further high resolution electron microscope (HRTEM) and energy-filtered transmission electron microscopy (EFTEM) observations confirmed the existence of the $Y_2Ti_2O_7$ phase and proved that these nano-oxides are in orientation relationship (OR) with the ferritic matrix [8–10]. The precipitation temperature determined by X-rays is about 1000 °C [2,3]. The addition of Ti was also shown to make the nano-oxides very resistant to coarsening, event at temperatures higher than 1100 °C [11]. In the aim to better understand the precipitation sequence in Y_2O_3 ODS Fe–18CrWTi alloys developed at CEA, the ODS steel powders (i.e. before the consolidation step) have been annealed at three temperatures 850 °C, 1100 °C and 1300 °C and observed by scanning electron microscopy (SEM) and transmission electron microscopy (TEM). We will show that the precipitation is more complex than expected and new phases have been discovered.

2. Experimental

For the SEM observations, the powders have been embedded in conductive resin and mechanically polished. A good surface quality for crystallographic back scatter electron (BSE) contrast and electron backscatter diffraction (EBSD) was obtained by a last polishing on a Buehler Vibromet II Table with non-crystalline silica. The TEM thin foils have been prepared by focus ion beam (FIB) on a FEI Strata400 equipment. The powders were deposed on a copper grid support with carbon glue and thinned by Ga^+ ion milling by decreasing

* Corresponding author. Tel.: +33 4 38 78 93 29.
E-mail address: cyril.cayron@cea.fr (C. Cayron).

0022-3115/$ - see front matter © 2010 Elsevier B.V. All rights reserved.
doi:10.1016/j.jnucmat.2010.01.023

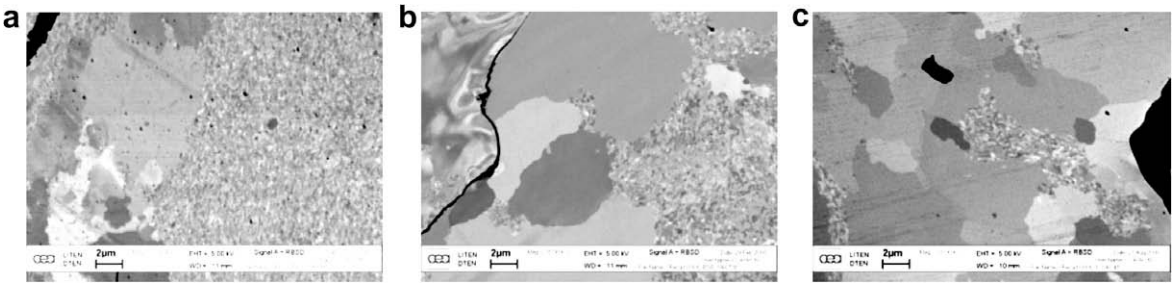

Fig. 1. SEM images with BSE of ODS steel powders annealed at (a) 850 °C, (b) 1100 °C and (c) 1300 °C.

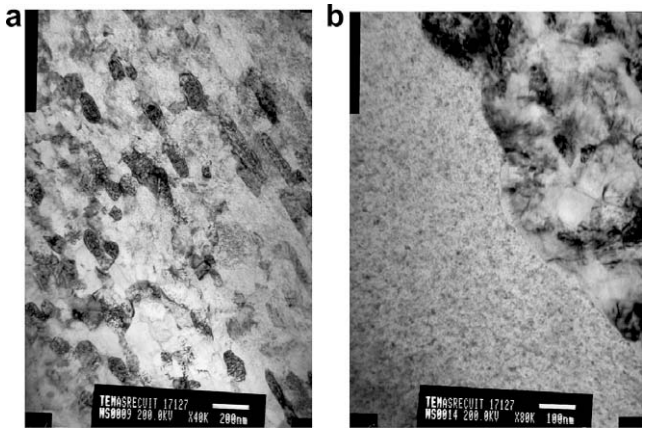

Fig. 2. TEM images in bright field mode of the ODS steel powders annealed at 850 °C and prepared by FIB. (a) In a small grain area and (b) at the frontier between a large grain (left, the small dark dots are FIB implantation defects) and a small grain area (right).

the voltage from 30 kV to 3 kV to avoid important Ga implantation in the TEM lamellas. Some powders have also been prepared by ultramicrotomy and by electropolishing.

The SEM images have been obtained on a LEO1530 FEG-SEM equipped with a Oxford/HKL EBSD acquisition system. The conventional TEM images, the selected area diffraction (SAED) and convergent beam electron diffraction (CBED) patterns have been acquired on a Jeol 2000FX microscope, the EFTEM images (Gatan Imaging Filter) on a Jeol 3010 microscope and the HRTEM images on a Jeol 4000EX microscope. All the equipments are located on the Nanocharacterization centre of Minatec (Grenoble).

3. Results

The ferritic grains show a bimodal structure with large grains (5–10 μm) and areas of small grains (100–200 nm) as illustrated in Fig. 1. The proportion of small grains decreases as the annealing temperature increases: it is 70% at 850 °C, 40% at 1100 °C and 10% at 1300 °C. The large grains probably absorb the small grains by abnormal grain growth. The EBSD maps (not presented here) do not show any particular texture; however, high frequency of special misorientations could be found such as rotations of 30° around <1 1 1>, and rotations of 58° around < 1 1 1>.

Whatever the TEM technique used to prepared the TEM samples (i.e. electropolishing, ultramicrotomy, or FIB) no precipitate could be detected in the ODS powders annealed at 850 °C, even at the frontier between the small grains and large grains (Fig. 2). The formation of Y–Ti–O nano-clusters between 850 °C and 1000 °C is however reported by small angle neutron scattering (SANS) in Refs. [11,12]. We conclude that if the precipitation has begun at 850 °C, the Y–Ti–O precipitates should have size lower than 2 nm and are not detectable in the Fe matrix by TEM.

In the powders annealed at 1100 °C, large precipitates (100–200 nm) were observed at the frontier between the small and large grains (Fig. 3). The SAED patterns, the EDS analysis and the EFTEM images (not presented here) prove that these precipitates correspond to the $Y_2Ti_2O_7$ phase (pyrochlore, Fd3m, a = 10.09 Å). Careful analysis of the SAED patterns acquired simultaneously on the precipitates and on the neighbour large grains reveals at least three special ORs (Table 1). We have checked with our software GenOVa [13] that these ORs are not redundant. Despite our efforts using conventional TEM, HRTEM and EFTEM, no nano-precipitates could be observed, neither at the grain boundaries nor inside the grains. Here again, we suspect that only nano-clusters (<2 nm) could be present. In general ODS steels elaborated or annealed at 1100 °C exhibit a high density of nano-oxides >10 nm, and it is not yet clear why they are not observed in our annealed powders.

The powders annealed at 1300 °C contain many types of micro and nano-precipitates. The powders prepared by electropolishing are not thin enough to be observed by TEM, but large hexagonal plates of size between 0.5 and 2 μm emerge from them. SAED and CBED patterns, and EDS (Fig. 4) prove that these precipitates correspond to the Y_2TiO_5 phase (hexagonal, a = 3.61 Å, c = 11.84 Å [14]). The presence of this phase was suspected in the ODS steels from X-ray diffractogram [2], but is the first time that this phase is clearly identified by TEM. Moreover, the strong link between Y_2TiO_5 and the pyrochlore $Y_2Ti_2O_7$ phase is demonstrated by the bright field image and the SAED patterns presented in Fig. 4d and e. The Y_2TiO_5 precipitates have grown on the $Y_2Ti_2O_7$ precipitates with the following epitaxy relationship:

$$\begin{cases} (004)Y_2TiO_5 = (222)Y_2Ti_2O_7 \\ (110)Y_2TiO_5 = (4\bar{4}0)Y_2Ti_2O_7 \end{cases}$$

According to this relation the theoretical lattice parameters are $a(Y_2TiO_5) = a(Y_2Ti_2O_7)/2\sqrt{2}$ = 3.56 Å and $c(Y_2TiO_5) = 2.a(Y_2Ti_2O_7)/\sqrt{3}$ = 11.65 Å, which is very close to those reported in [14]. The existence of a phase transformation between the hexagonal and cubic forms of Dy_2TiO_5 with lattice parameters close to those of Y_2TiO_5 and $Y_2Ti_2O_7$ has been reported in [15]. Therefore, it is possible that some of the $Y_2Ti_2O_7$ precipitates observed at 1100 °C have been transformed into Y_2TiO_5 precipitates at 1300 °C.

The powders annealed at 1300 °C contain also a dense precipitation of nano-oxides with spherical or facetted shapes of sizes around 20–30 nm. These precipitates clearly appear in the EFTEM images with a slit at 547 eV (Fig. 5). Most of them contain O, Ti and Y homogeneously distributed without any core/shell structure, with a Y/Ti atomic ratio estimated from the EDS Y(Kα) and Ti(Kα) peaks to be between 2.5 and 3.5. Those that are oriented in diffraction conditions are also visible by HRTEM (Figs. 6 and 8). More than

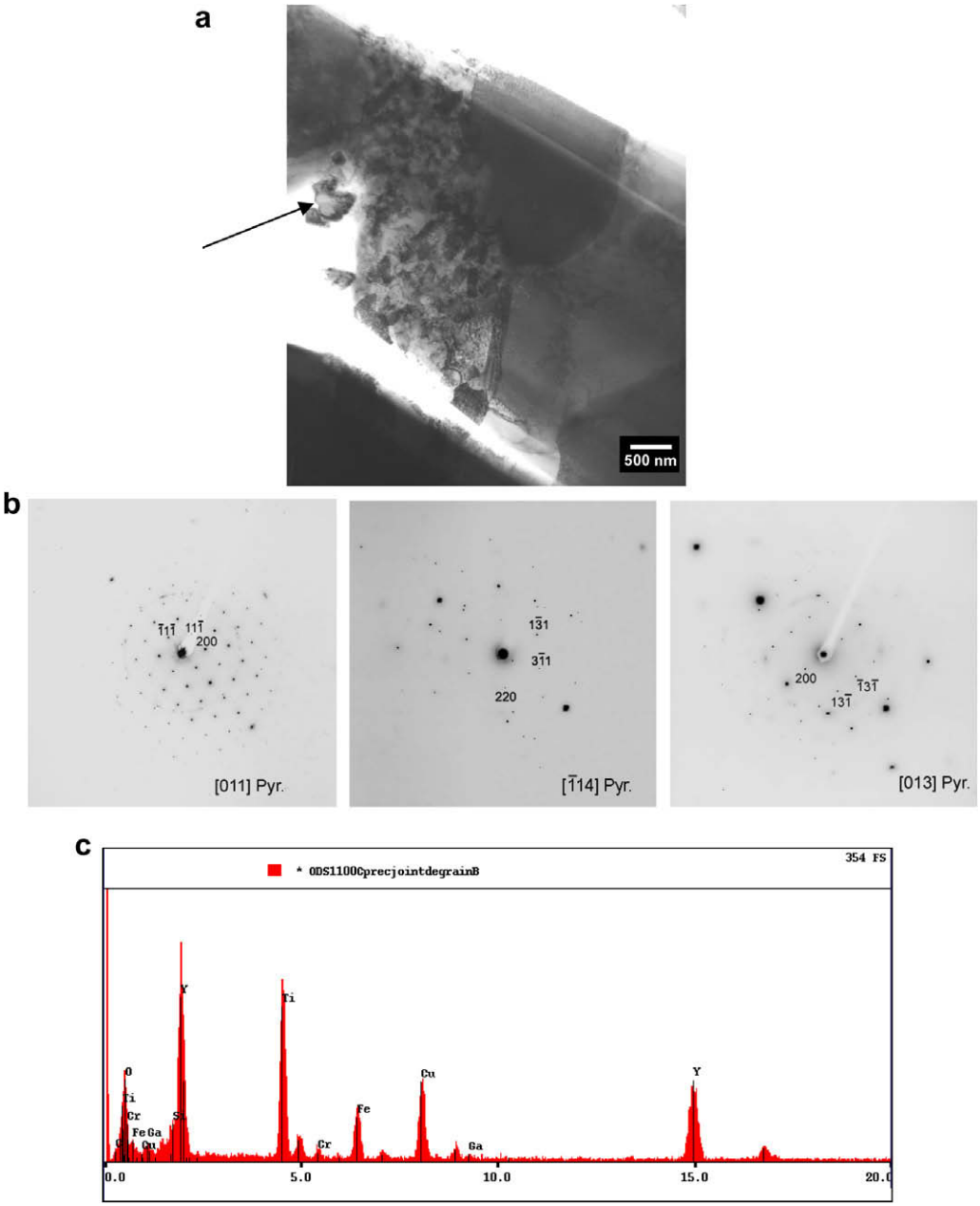

Fig. 3. ODS steel powder annealed at1100 °C. TEM sample prepared by FIB. (a) Agglomerate of three $Y_2Ti_2O_7$ phase (pyrochlore) precipitates (see arrow) of about 100 nm at the frontier between a small grain region and a large ferritic grain. (b) SAED patterns of one precipitate. (c) The EDS spectrum confirms the presence of Y, Ti and O.

Table 1
Three orientation relationships between the pyrochlore $Y_2Ti_2O_7$ and the Fe matrix. OR 3 is similar to the Kurdjumov–Sachs OR classically observed in martensite.

OR 1	OR 2	OR 3
[$\bar{1}$ 1 1] Feα // [2 $\bar{3}$ 1] Pyr.	[0 0 1] Feα // [2 $\bar{3}$ 1] Pyr.	[$\bar{1}$ 1 1] Feα // [0 1 1] Pyr.
(1 1 0) Feα // (3 1 $\bar{3}$) Pyr.	(1 $\bar{1}$ 0) Feα // (1 1 1) Pyr.	(1 1 0) Feα // (1 1 $\bar{1}$) Pyr.

twenty nano-oxides have been imaged and indexed, and all of them except one could be classified among the three following phases:

- 20% correspond to the Y_2O_3 phase (Fig. 6).
- 20% correspond to the $Y_2Ti_2O_7$ phase (Fig. 7).
- 60% correspond to a new phase never reported before (Fig. 8).

There is no ambiguity for indexing the power spectra between the cubic Y_2O_3 and $Y_2Ti_2O_7$ phases because the former is BCC Ia3 (a = 10.60 Å) and the latter is FCC Fd3m (a = 10.09 Å). We have tried to identify the new phase by assuming that it is a superstructure of the pyrochlore $Y_2Ti_2O_7$ phase. Firstly, we have tried a hexagonal structure, that we will call temporarily PyrHex, with lattice parameters $a_{PyrHex} = a(Y_2Ti_2O_7)/\sqrt{2} = 7.14$ Å and $c_{PyrHex} = \sqrt{3}(Y_2Ti_2O_7) = 18.2$ Å. This structure was in agreement with about 70% of the HRTEM images of the unknown phase. Then, we have tried more complex structures and discovered one in agreement with all the images. We called the new phase PyrOrtho. The structure is orthorhombic with lattice parameters $a_{PyrOrtho} = a_{PyrHex} = a(Y_2Ti_2O_7)/\sqrt{2} = 7.14$ Å, $b_{PyrOrtho} = \sqrt{3}a_{PyrHex} = \sqrt{3}/2a(Y_2Ti_2O_7) = 12.4$ Å and $c_{PyrOrtho} = c_{PyrHex} \approx \sqrt{3}a(Y_2Ti_2O_7)$ (=17.5 Å) = 18.2 Å. Some of the PyrOrtho precipitates are twinned by a rotation of 180° around the $[1\,1\,2]_{PyrOrtho}$ axis (Fig. 9).

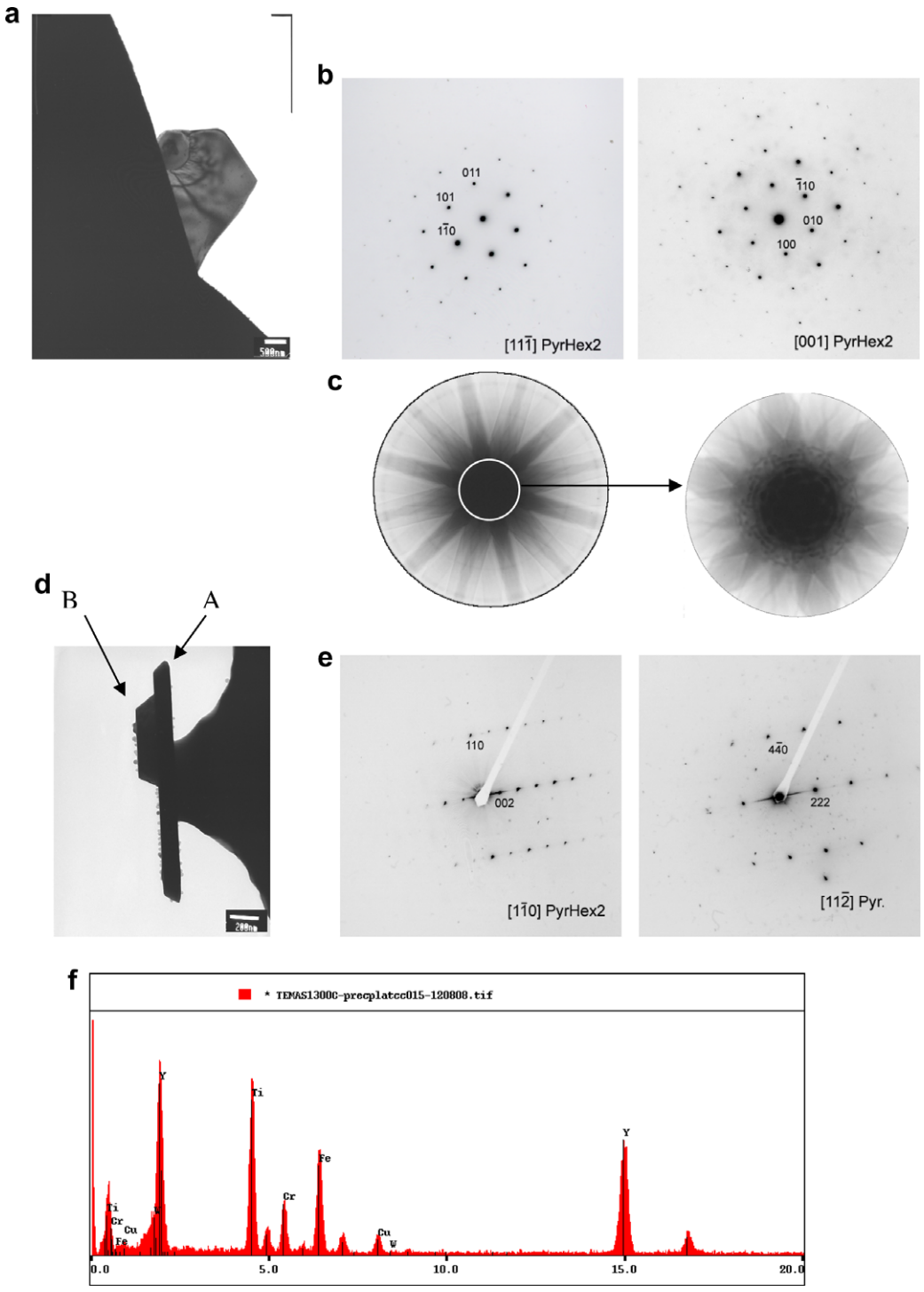

Fig. 4. ODS steel powder annealed at1300 °C. TEM sample prepared by electropolishing. The powders are not thin enough but numerous large hexagonal plate-shaped precipitates (1 μm) emerge from them (called here PyrHex2). (a) One precipitate lying flat with (b) two SAED patterns and (c) a CBED pattern proving the hexagonal symmetry of the structure. (d) Another precipitate on the edge (noted A) lying on a pyrochlore $Y_2Ti_2O_7$ precipitate (noted B) with (e) SAED patterns of the two precipitates showing an orientation relationship between the two structures. (f) EDS spectrum. Our analysis proves that hexagonal precipitates PyrHex2 are Y_2TiO_5.

4. Conclusions

Fe–18CrWTi Y_2O_3 ODS powders have been annealed at 850 °C, 1100 °C and 1300 °C and their microstructure has been studied by SEM and TEM. The powders are constituted of large micrometric grains and nanometric ferritic grains. The proportion of the nanograins decreases with the annealing temperature. At 850 °C, the samples appear to be free of any precipitates. Nano-clusters <2 nm are however probably present. At 1100 °C some precipitates of several hundreds of nanometres are detected at the grains boundaries and identified to the $Y_2Ti_2O_7$ pyrochlore phase. Here again, the nano-oxides could not be detected. At 1300 °C, the precipitation has greatly changed. The sample contains hexagonal plate-shaped precipitates of size

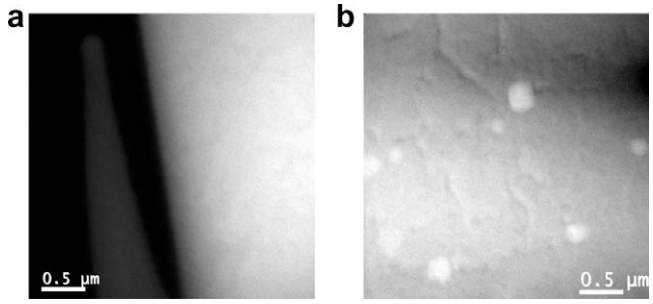

Fig. 5. EFTEM images with a slit at 547 eV (oxygen) of the ODS steel powders annealed at (a) 1100 °C and (b) 1300 °C. TEM samples prepared by FIB. The nano-oxides are not visible in (a) whereas they appear clearly in (b).

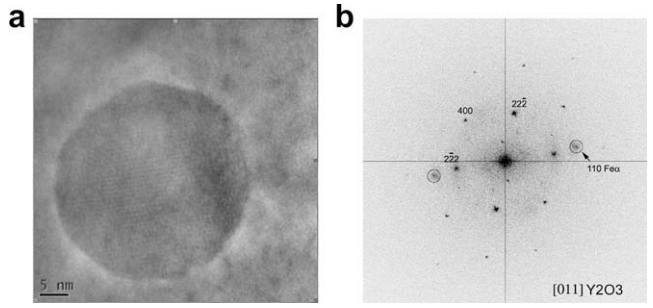

Fig. 6. Nano-oxide in the ODS steel powders annealed at 1300 °C prepared by FIB. (a) HRTEM image and (b) power spectrum proving without ambiguity the Y_2O_3 structure.

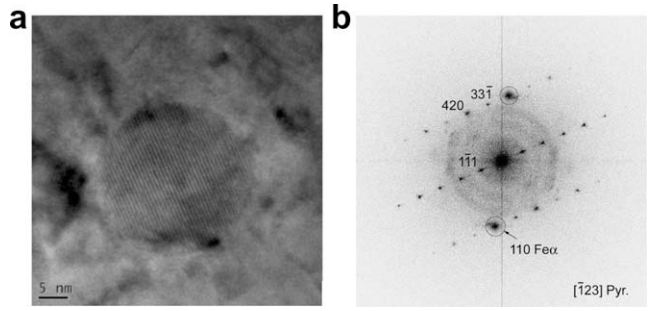

Fig. 7. Nano-oxide in the ODS steel powders annealed at 1300 °C prepared by FIB. (a) HRTEM image and (b) power spectrum proving without ambiguity the $Y_2Ti_2O_7$ pyrochlore structure.

between 0.5 and 1 µm. Their structure is hexagonal with lattice parameters $a = 3.56$ Å and $c = 11.65$ Å; it corresponds to the Y_2TiO_5 phase. Moreover, a high density of rounded and facetted nano-oxides of size around 20–30 nm could be imaged by EFTEM and HRTEM. They are of different types: Y_2O_3, $Y_2Ti_2O_7$ and a new phase containing Y, Ti and O that we called PyrOrtho. This structure seems to be a complex and ordered mixture of the Y_2O_3 and pyrochlore phases. It is orthorhombic with lattice parameters $a = 7.24$ Å, $b = 12.4$ Å and $c = 18.2$ Å. It has never been reported before and its existence will have to be confirmed. This study shows that the addition of Ti during the elaboration of the Y_2O_3 ODS steels makes the precipitation sequence more complex that was believed. The results are summarized in Table 2.

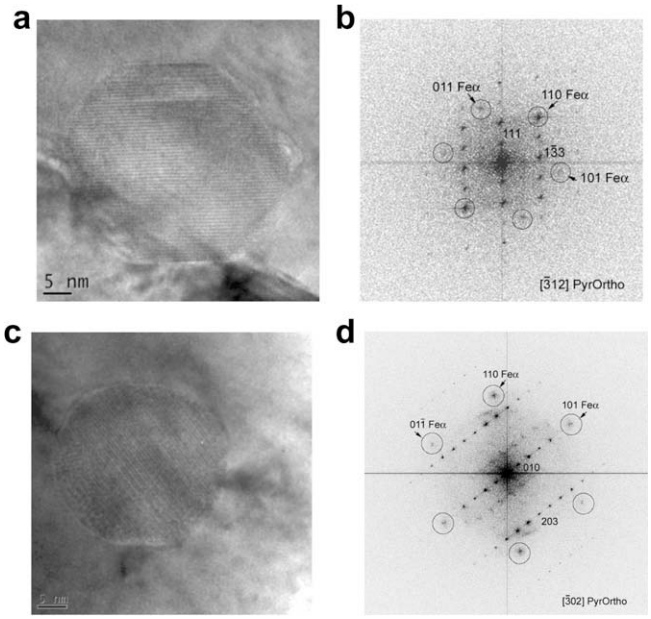

Fig. 8. Nano-oxides in the ODS steel powders annealed at1300 °C prepared by FIB. (a) and (c) HRTEM images (b) and (d) power spectra. They are not in agreement with the structures Y_2O_3, $Y_2Ti_2O_7$ nor Y_2TiO_5. Actually, these nano-oxides are an orthorhombic surstructure of the pyrochlore phase that we called PyrOrtho.

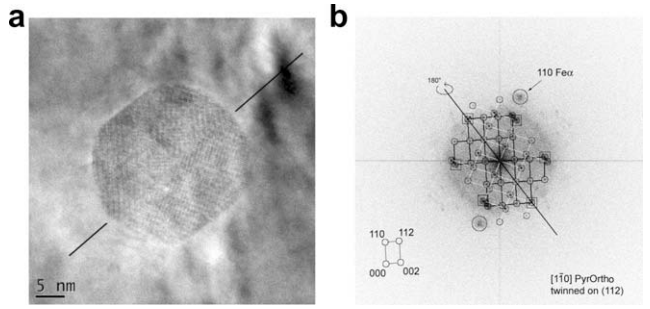

Fig. 9. A twinned PyrOrtho nano-oxide in the ODS steel powders annealed at 1300 °C and prepared by FIB. (a) HRTEM image and (b) power spectrum. The twin corresponds to a 180° rotation around the common $[1\ 1\ 2]_{PyrOrtho}$ axis.

Table 2
Summary of the SEM and TEM observations in the annealed ODS powers.

After milling	Anneal at 850 °C	Anneal at 1100 °C	Anneal at 1300 °C
• Ferritic nanograins	• Bimodal structure of the ferritic grains. Nanograins = 70%	• Bimodal structure of the ferritic grains. Nanograins = 40%	• Bimodal structure of the ferritic grains. Nanograins = 10%
• No nano-oxide visible by TEM. The Y_2O_3 particles have been dissolved by the milling[2–5]. Possible presence of nano-clusters (<2 nm) [11]	• No nano-oxide visible by TEM. Possible presence of nano-clusters (<2 nm) [11]	• No nano-oxide visible by TEM. Possible presence of nano-clusters (<2 nm).	• Dense formation of nano-precipitates (10–30 nm) of Y_2O_3, $Y_2Ti_2O_7$ and a new phase called PyrOrtho
		• $Y_2Ti_2O_7$ precipitates at grain boundaries (100–200 nm)	• Numerous hexagonal Y_2TiO_5 plates (0.5–2 µm)

References

[1] Y. de Carlan, J.L. Bechade, P. Dubuisson, J.L. Seran, P. Billot, A. Bougault, T. Cozzika, S. Doriot, D. Hamon, J. Henry, M. Ratti, N. Lochet, D. Nunes, P. Olier, T. Leblond, M.H. Mathon, J. Nucl. Mater. 386–388 (2009) 430.
[2] T. Okuda, M. Fujiwara, J. Mater. Sci. Lett. 14 (1995) 1600.
[3] Y. Kimura, S. Takaki, S. Suejima, R. Uemori, H. Tamahiro, ISIJ Int. 39 (1999) 176.
[4] S. Ukai, S. Mizuta, M. Fujiwara, T. Okuda, T. Kobayashi, J. Nucl. Sci. Technol. 39 (2002) 778.
[5] C. Cayron, E. Rath, I. Chu, S. Launois, J. Nucl. Mater. 335 (2004) 83.
[6] M. Klimenkov, R. Lindau, A. Möslang, J. Nucl. Mater. 386–388 (2009) 553.
[7] S. Ukai, M. Harada, H. Okada, M. Inoue, S. Nomura, S. Shikakura, K. Asabe, T. Nishida, M. Fujiwara, J. Nucl. Mater. 204 (1993) 65.
[8] M. Klimiankou, R. Lindau, A. Möslang, J. Nucl. Mater. 329–333 (2004) 347.
[9] S. Yamashita, S. Ohtsuka, N. Akasaka, S. Ukai, S. Ohnuki, Phil. Mag. Lett. 84 (2004) 525.
[10] K. Oka, S. Ohnuki, S. Yamashita, N. Akasaka, S. Ohtsuka, H. Tanigawa, Mater. Trans. 48 (2007) 2563.
[11] M. Ratti, D. Leuvrey, M.H. Mathon, Y. de Carlan, J. Nucl. Mater. 386–388 (2009) 540.
[12] M.J. Alinger, G.R. Odette, D.T. Hoelzer, Acta Mater. 57 (2009) 392.
[13] C. Cayron, J. Appl. Cryst. 40 (2007) 1179.
[14] N. Mizutani, Nippon Kagaku Kaishi, J. Chem. Soc. Jpn. (1974) 1623.
[15] Y.F. Shepelev, M.A. Petrova, Russ. J. Inorg. Chem. 51 (2006) 1636.